ChemComm

Accepted Manuscript

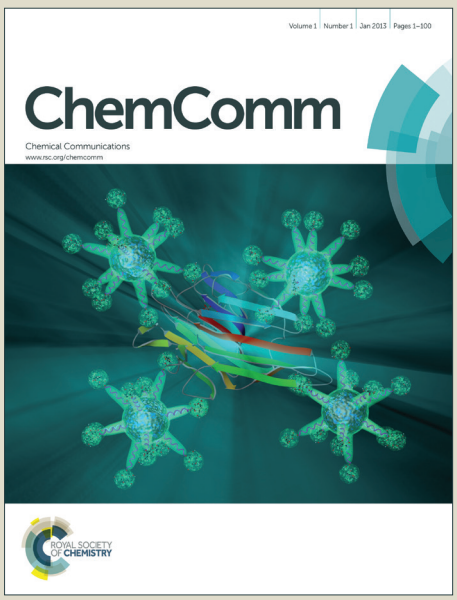

ROYAL SOCIETY OF CHEMISTRY

www.rsc.org/chemcomm

Journal Name

RSCPublishing

COMMUNICATION

Enhanced Photovoltaic Performance of Perovskite $CH_3NH_3PbI_3$ Solar Cells with Free Standing TiO_2 Nanotube Array Films

Cite this: DOI: 10.1039/xoxxoooooox

Received ooth January 2012,
Accepted ooth January 2012

DOI: 10.1039/xoxxoooooox

www.rsc.org/

Xianfeng Gao, Jianyang Li, Joel Baker, Yang Hou, Dongsheng Guan, Junhong Chen, Chris Yuan*

Free standing TiO_2 nanotube array films are fabricated and first applied as electrodes in perovskite $CH_3NH_3PbI_3$ sensitized solar cells. The device demonstrates improved light absorption with more than 90% of light absorbed in the whole visible range and reduced charge recombination rate, leading to a significant improvement of the photocurrent and efficiency. This study suggests a promising way of improving the conversion efficiency of perovskite solar cells through novel electrode.

The development of organometallic halide perovskite sensitizers has attracted enormous attention on solar cell applications due to their excellent light absorbing characteristics. [1] Perovskite materials were first used as sensitizers to replace traditional organic dye molecules in dye sensitized TiO_2 nanocrystalline solar cells with iodide based electrolyte. These cells initially obtained an efficiency in the range of 3.7-6.5%. [2] In 2012, the application of $CH_3NH_3PbI_3$ leads to a breakthrough on the solid-state dye sensitized solar cell (DSSC), with a power conversion efficiency of 9.7% obtained using submicrometer thick mesoporous TiO_2 film electrode sensitized by perovskite $CH_3NH_3PbI_3$ nanocrystals with spiro-MeOTAD as hole conductors.[3] At the same time, extensive research has been conducted on the development of high efficiency solid state solar cells, with a high efficiency of 10%-15% achieved. [4]

The primary advantage of the perovskite absorbers is their direct bandgap with large absorption coefficients over a broad range, which enables efficient light absorption in ultra-thin films. However, when only considering the light harvesting efficiency, perovskite based devices still has large potential to be improved in terms of light management. Simulated results indicate that solar cells can obtain a photocurrent of 27.2 mA/cm^2 if the total photons in 280-800 nm could be used to generate electricity,[5] while current perovskite solar cells only obtain photocurrent around 20 mA/cm^2 on thin film solid state solar cells[6] and no more than 16 mA/cm^2 on iodide electrolyte based solar cells.[2] The light absorption spectrum indicates that a $CH_3NH_3PbI_3$ sensitized electrode appears to be more efficient to absorb light below 500nm. The absorbance decreases gradually from 500 to 800 nm when applied on nanoparticle electrodes.[6, 7] Proper material selection and engineering design for light management both need to be optimized to increase the photocurrent and the conversion efficiency.

In this paper, $CH_3NH_3PbI_3$ sensitized perovskite solar cells are fabricated using free standing TiO_2 nanotube array electrode. The perovskite absorber was infiltrated into the TiO_2 nanotube successfully. With the new TiO_2 nanotube electrode, a significant improvement of light absorption was obtained, showing over 90% light absorption in the whole visible range. Combining the effect from a reduced recombination rate, the TiO_2 nanotube based perovskite solar cells show a significant increase of the power conversion efficiency over the conventional nanoparticle based solar cells. In this study, the dependence of light absorption and photovoltaic performance with iodide liquid electrolytes on the nanotube length was also investigated, while the solid state hole conductors were not employed in order to avoid variations in the pore-filling fraction, which will otherwise complicate the electron recombination analysis.[8] The device obtained a high photocurrent density of 17.9 mAcm^{-2} using iodide liquid electrolyte and a conversion efficiency of 6.52%. The results indicate that TiO_2 nanotubes could be a promising perovskite host for enhancing the light absorption near its energy band edge, and can potentially pave a way for novel perovskite solid state solar cell designs and fabrications.

Here freestanding TiO_2 nanotube (TNT) arrays were prepared by a two-step anodization process and then detached from the substrate with in-situ field-assisted chemical dissolution.[9] After transferring the free standing nanotube arrays to FTO which was covered by a spin-coated TiO_2 blocking layer, a sequential deposition approach was used to deposit the perovskite absorber into the nanotubes. PbI_2 crystals were deposited into the nanotubes by spin coating of 1M PbI_2 solution in N,N-dimethylformamine. For perovskite formation, the TNT/PbI_2 film was immersed into a solution of CH_3NH_3I in 2-propanol. In an attempt to increase the deposition of the perovskite absorber on the high aspect ratio TiO_2 structure, a relatively high concentration (30 mg ml^{-1}) of CH_3NH_3I was used, which tends to form $CH_3NH_3PbI_3$ with small particle size and fits the pore size of nanotube arrays. It was observed that a low concentration of CH_3NH_3I will result in formation of crystals with sizes typically larger than 500 nm, which may block the pores and hamper the transformation of PbI_2 inside the nanotubes. In this case, the formed perovskite crystals settle on the surface of the nanotube arrays and

an inefficient sensitized electrode is produced. Further experimental details are provided in Electronic Supplementary Information.

The formation of perovskite in the nanotube arrays was tracked by X-ray diffraction (XRD) spectroscopy (Figure 1). When the PbI_2 crystals were deposited into the nanotube, two additional peaks appear at approximately 12.72 and 39.52 degrees, respectively, corresponding to the reflection from (101) and (110) lattice planes of hexagonal polytype (JCPDS 07-0235). After the transformation process from PbI_2 to $CH_3NH_3PbI_3$ was completed, a series of new diffraction peaks related to a tetragonal perovskite structure were observed. The strong peaks located at 14.20, 19.78, 28.23, 28.52, 29.80, 31.95, 40.61 and 43.20 degrees correspond to the reflections from (110), (112), (004), (220), (310), (312), (224) and (314) lattice planes of the tetragonal perovskite structure.[2, 10] No impurity peaks appear in both steps, suggesting a complete formation of PbI_2 and its controlled transformation to $CH_3NH_3PbI_3$. The final perovskite absorber is well crystallized and the phase is pure.

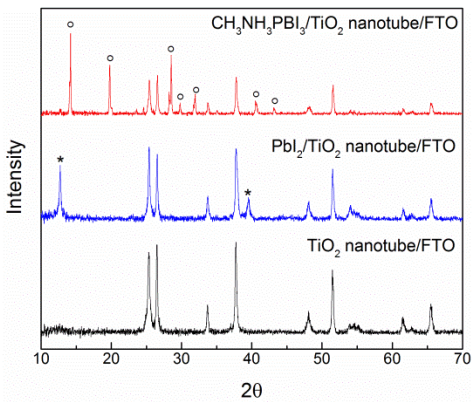

Figure 1. XRD spectra of pristine TiO_2 nanotube electrode (a), PbI_2/TiO_2 nanotube electrode (b) and $CH_3NH_3PbI_3/TiO_2$ nanotube electrode (c). PbI_2 and $CH_3NH_3PbI_3$ peaks are marked with star and circle respectively.

Figure 2 compares the morphology of TiO_2 nanotube electrode before and after the perovskite dye deposition using the scanning electron microscopy (SEM) and transmission electron microscopy (TEM) images. Figure 2a shows a typical surface morphology of the as prepared TiO_2 nanotube arrays. After the two step anodization, a porous thin layer was formed on top of the nanotube array, which protects the nanotube arrays from top end bundling and avoids the cracks during the detachment and film transfer process (Figure 2a). This provides a safe way to get ultrathin free standing TiO_2 nanotube array film. It is worth noting that the surface porous layer is connected with the underlayer tube opening (Figure S1), which

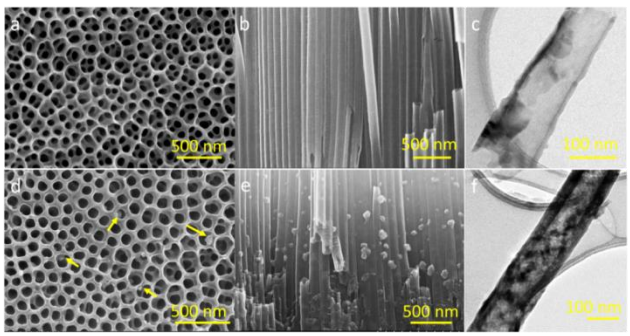

Figure 2. Morphology characterization of TiO_2 nanotube before and after the perovskite dye deposition. Figure a-c show SEM images of top view (a), cross section image (b) and TEM image (c) of pristine TiO_2 ;Figure d-f show SEM images of top view (d), cross section image (e) and TEM image (f) of TiO_2 nanotube with $CH_3NH_3PbI_3$ deposition.

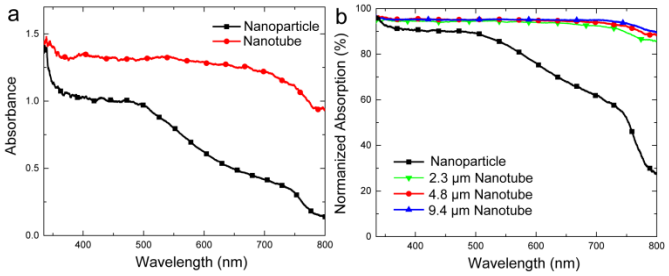

Figure 3. (a) UV-Vis absorption of $CH_3NH_3PbI_3$ sensitized TiO_2 nanoparticle and TiO_2 nanotube electrode. (b) Normalized adsorption spectra as a function of TiO_2 nanotube thickness with comparison with TiO_2 nanoparticle electrode.

would not affect the following perovskite deposition process. To investigate the dependence of the photovoltaic performance on the film thickness, three types of TiO_2 nanotube array films were prepared with the tube length controlled at 2.3 μm, 4.8 μm, and 9.4 μm during the anodization process (Figure S2). Figure 1b shows the cross section image of the nanotube arrays, indicating a well-controlled nanotube structure formed. After the perovskite absorber deposition, the nanotube structure remains intact. It is shown that some nanoparticles attached on the edge of the nanotube, and the formation of the perovskite absorber did not block the pores (Figure 2d). Cross-sectional SEM images and TEM images (Figure 2e-2f) indicate a successful infiltration of the perovskite absorber into the nanotubes. The particle sizes of $CH_3NH_3PbI_3$ were limited to less than 100nm as controlled by the pore size of the nanotube. Cross-sectional EDS mapping (Figure S3) indicates Pb and I are well distributed along the nanotubes array film. Weight percentages for Pb and I from EDS elemental analysis are found at 5.22% and 10.11%, respectively, which corresponds to a 0.78% and 2.47% atomic ratio and indicates a good stoichiometric ratio of Pb to I in the obtained perovskite $CH_3NH_3PbI_3$.

Figure 3a shows typical ultraviolet-visible (UV-Vis) absorption spectrum of $CH_3NH_3PbI_3$ sensitized 4.8 μm TiO_2 nanotube array electrode. For comparison, a spectrum of photoelectrode based on TiO_2 nanoparticle film with the same thickness was presented. When compared, the nanotube based electrodes have significantly larger absorbance of visible light over the whole spectrum than nanoparticle based electrodes. The nanoparticle based electrodes appear to be efficient to absorb light below 500nm. The absorbance decreases gradually from 500 to 800 nm, which is consistent with previously reported results.[15, 16] With TiO_2 nanotubes as the perovskite host, the absorbance is clearly improved, especially in the long wavelength region, which could contribute to the enhanced light trapping ability of the nanotube array. The enhanced light absorption will help generate the photo excited electrons and eventually improve the power conversion efficiency. Note that the scale in the figure is optical density, where an absorbance of ~1 corresponds to ~90% light absorption. Figure 3b presents corresponding absorption characteristics of both nanoparticle and nanotube electrodes, where nanotube electrodes show over 90% of light absorption in almost the full visible light region. Figure 3b also presents the dependence of the light absorption on the nanotube length. It is interesting to observe that when the TiO_2 nanotube length increases from 2.3 μm to 9.4 μm, the absorption is only slightly increased in the 600-800 nm region, which could be related to the overall strong absorption of $CH_3NH_3PbI_3$ sensitized TiO_2 nanotube electrodes. It is worth noting that even with 2 μm nanotube arrays, the photoelectrode shows a very high light absorption. The results indicate that TiO_2 nanotubes could be a promising host for $CH_3NH_3PbI_3$ solar cells with significant light absorption

enhancement effects, which is important in design of high efficiency solar devices and provides a new route to improve current perovskite solar cell technology.

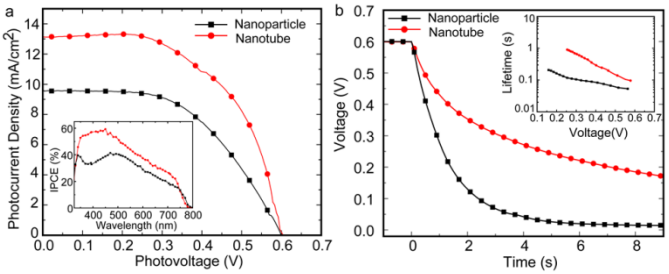

Figure 4. (a) J-V curves, IPCE (inset of image a), (b)open-circuit voltage decay and electron lifetimes (inset of image b) of the perovskite solar cell with nanoparticle electrode and TNT film electrode.

Figure 4a shows the current-voltage curves of perovskite solar cell based on TiO_2 nanoparticle and TiO_2 nanotube array films under AM1.5 illumination. A photo conversion efficiency of 4.46% is obtained on the 4.8 μm TiO_2 nanotube electrode, resulting from a photocurrent density (J_{SC}) of 13.1 mA/cm^2, open-circuit voltage (V_{OC}) of 0.60V and fill factor of 0.568. Notice that the J-V curve is obtained under reverse scan with a slow scan speed, which can minimize the efficiency deviation under different scan directions[11] (Figure S4 and Table S1). In comparison, on the nanoparticle electrode with the same thickness, the cell efficiency is only 2.99% with a photocurrent density (J_{SC}) of 9.5 mA/cm^2, open-circuit voltage (V_{OC}) of 0.60V and fill factor of 0.525. In our tests, TiO_2 nanotube based device also presents higher incident photo to current efficiency (IPCE) at all effective photo response region (inset of Figure 4a). It indicates that using TiO_2 nanotubes as the electrode host results in a significant photocurrent increase and thus an obvious photo conversion efficiency improvement.

To understand the effect of TiO_2 nanotube array on the improved photovoltaic performance, photovoltage decay measurements were performed to investigate the charge transport and recombination properties of the TiO_2 nanotube based perovskite photoelectrode (Figure 4b). Briefly, the electron lifetimes (τ_n) could be derived from the photovoltage decay curve according to,[12]

$$\tau_n = \frac{k_B T}{q}\left(\frac{dV_{OC}}{dt}\right)^{-1}$$

Where k_B is the Boltzmann constant, T is the absolute temperature, and q is the positive elementary charge. Figure 4b shows the photovoltage decay plots and the electron lifetimes as a function of photovoltage (inset). It is observed that the photovoltage of the TiO_2 nanotube array electrode decays slower than that of the TiO_2 nanoparticle electrode, which also presents a longer electron life time at equal potentials. The decreased electron life time of the TiO_2 nanoparticle electrode means a higher charge recombination rate and a lower charge collection efficiency than those of the TiO_2 nanotube electrode.[13] These results indicate that the enhancement of TiO_2 nanotube based perovskite solar cells is attributed to both the enhanced light absorption and the reduced charge recombination.

To investigate the potential of TiO_2 nanotubes as a host for perovskite solar cells, the dependence of photovoltaic performance on the nanotube film thickness was also studied (Table 1). It is found that the device performances show strong dependence on nanotube length. A photo conversion efficiency of 6.52% is obtained, resulting from a 2.3 μm nanotube array film with a photocurrent density (J_{SC}) of 17.9 mA/cm^2, open-circuit voltage (V_{OC}) of 0.63V and fill factor of 0.578. The device efficiency is among the best results reported on perovskite solar cells using a liquid electrolyte.[2, 7] Considering that additional surface treatment was not performed and the device parameters were not fully optimized, this result is very encouraging. Table 1 shows the J_{SC} values between 17.9 mAcm^{-2} to 9.73 mAcm^{-2} when the nanotube length changes from 2.3 μm to 9.4 μm. The V_{OC} also decreases from 0.63 V to 0.54V with the increasing of TiO_2 nanotube length. As a result, the photo conversion efficiency decreases from 6.52% to 3.26% when the TiO_2 nanotube film thickness increases from 2.3 μm to 9.4 μm.

Table 1. Photocurrent-Voltage characteristics of the perovskite solar cell with varied thickness TNT film under AM1.5 irradiation.

	V_{OC} [V]	J_{SC} [mAcm^{-2}]	FF	η [%]
2.3 μm	0.63	17.9	0.578	6.52
4.8 μm	0.60	13.1	0.568	4.46
9.4 μm	0.54	9.7	0.624	3.26

Considering the thickness of the TiO_2 nanotube film only has slight effect on the light absorption due to the overall high absorption ability, it is concluded that charge collection efficiency governs the performance of the TiO_2 nanotube based perovskite solar cells. Photovoltage decay measurements (Figure S5) show that the photovoltage of the short nanotube array film electrode decays slower, which also presents a longer electron life time at equal potentials. The decreased electron life time of the long nanotube film suggests a high charge recombination rate and relatively low charge collection efficiency, which consequently limits the photo conversion efficiency of the devices. IPCEs (Figure S6) of shorter nanotube based devices show significant higher quantum efficiency resulting from the higher charge collection efficiency, which is consistent with photovoltage decay measurement. Since the electron collection efficiency is close to 100% under short circuit conditions even for 20 μm thick nanotube arrays,[14] it is therefore reasonable to predict that a higher recombination rate may be due to the restrained regeneration of the oxidized dyes, which is related to excited hole extraction. To get a stable performance, low concentration I^- electrolyte was used here to restrain the dye bleaching,[7] which will also result in a less effective regeneration of the oxidized dyes and lead to an increased electron recombination.[15] When the length of TiO_2 nanotube increases, the I^- diffusion pathway is prolonged, resulting in an enhanced I^- depletion level inside the nanotubes, and subsequently an acceleration of the recombination.[15] It should be noted that the long term stability of nanotube based device is still not good because of the chemical instability of perovskite in the iodide electrolyte. Similar to other liquid perovskite solar cells, the degradation of the cell performance is accompanied by perovskite blenching in iodide electrolyte. To improve their long term stability and fully utilize the advantage of nanotube structure, development of TiO_2 nanotube based solid state perovskite solar cells is currently in progress.

In summary, pervoskite solar cells based on free standing TiO_2 nanotube arrays are developped, which presents an improved photovoltaic performance with enhanced photocurrent and increased power conversion efficiency. The improvement is not only applicable to the boosting of light absorption, but also contributes to the reduced charge combination in nanotube electrodes, which suggests TiO_2 nanotube arrays could be a promising perovskite host to improve the efficiency further. It is also found the photovoltaic performance increases with the decreasing of the TiO_2 nanotube film thickness, attibuting to the different photoexcited charge extraction and collection efficiencies. An encouraging photovoltaic

performance with 17.9 mA/cm^2 photocurrent and 6.52% efficiency was shown by the solar cell with 2.3 μm TiO_2 nanotubes. Considering the feasibility of short nanotubes to provide uniform hole transport material deposition without losing light absorption enhancement features, the well aligned TiO_2 nanotube array films could be a promising electrode for high efficiency solid state perovskite solar cells fabrication.

Notes and references

[a] Department of Mechanical Engineering, University of Wisconsin Milwaukee, Wisconsin, 53211, United States, E-mail: cyuan@uwm.edu

Electronic Supplementary Information (ESI) available: Experimental details, Cross section images of free standing TiO_2 nanotube array, EDS maping of TiO_2/perovskite film and photovoltage decay measurement and IPCE of TiO_2 nanotube devices with varied thickness are available. See DOI: 10.1039/c000000x/

1. B. V. Lotsch, *Angew Chem Int Ed Engl*, 2014, **53**, 635-637; H. J. Snaith, *The Journal of Physical Chemistry Letters*, 2013, **4**, 3623-3630; P. V. Kamat, *The Journal of Physical Chemistry Letters*, 2013, **4**, 3733-3734; J. Bisquert, *The Journal of Physical Chemistry Letters*, 2013, **4**, 2597-2598.
2. J. H. Im, C. R. Lee, J. W. Lee, S. W. Park and N. G. Park, *Nanoscale*, 2011, **3**, 4088-4093.
3. H. S. Kim, C. R. Lee, J. H. Im, K. B. Lee, T. Moehl, A. Marchioro, S. J. Moon, R. Humphry-Baker, J. H. Yum, J. E. Moser, M. Gratzel and N. G. Park, *Scientific reports*, 2012, **2**, 591.
4. B. Conings, L. Baeten, C. De Dobbelaere, J. D'Haen, J. Manca and H. G. Boyen, *Adv Mater*, 2013; D. Liu and T. L. Kelly, *Nat Photon*, 2014, **8**, 133-138; J. Burschka, N. Pellet, S. J. Moon, R. Humphry-Baker, P. Gao, M. K. Nazeeruddin and M. Gratzel, *Nature*, 2013, **499**, 316-319; M. Liu, M. B. Johnston and H. J. Snaith, *Nature*, 2013, **501**, 395-398; K. Wojciechowski, M. Saliba, T. Leijtens, A. Abate and H. J. Snaith, *Energy & Environmental Science*, 2014, **7**, 1142-1147; Q. Chen, H. Zhou, Z. Hong, S. Luo, H.-S. Duan, H.-H. Wang, Y. Liu, G. Li and Y. Yang, *Journal of the American Chemical Society*, 2013, **136**, 622-625.
5. G. P. Smestad, F. C. Krebs, C. M. Lampert, C. G. Granqvist, K. L. Chopra, X. Mathew and H. Takakura, *Solar Energy Materials and Solar Cells*, 2008, **92**, 371-373.
6. M. M. Lee, J. Teuscher, T. Miyasaka, T. N. Murakami and H. J. Snaith, *Science*, 2012, **338**, 643-647.
7. Y. Zhao and K. Zhu, *The Journal of Physical Chemistry Letters*, 2013, **4**, 2880-2884.
8. H. S. Kim, J. W. Lee, N. Yantara, P. P. Boix, S. A. Kulkarni, S. Mhaisalkar, M. Gratzel and N. G. Park, *Nano letters*, 2013, **13**, 2412-2417.
9. H. M. Ouyang, G. T. Fei, Y. Zhang, H. Su, Z. Jin, S. H. Xu and L. De Zhang, *Journal of Materials Chemistry C*, 2013, **1**, 7498-7506.
10. T. Baikie, Y. Fang, J. M. Kadro, M. Schreyer, F. Wei, S. G. Mhaisalkar, M. Graetzel and T. J. White, *Journal of Materials Chemistry A*, 2013, **1**, 5628.
11. K. Naoki, C. Yasuo and H. Liyuan, *Japanese Journal of Applied Physics*, 2005, **44**, 4176; M. Herman, M. Jankovec and M. Topič, *International Journal of Photoenergy*, 2012, **2012**, 1-11.
12. A. Zaban, M. Greenshtein and J. Bisquert, *Chemphyschem : a European journal of chemical physics and physical chemistry*, 2003, **4**, 859-864.
13. K. Zhu, N. R. Neale, A. Miedaner and A. J. Frank, *Nano letters*, 2006, **7**, 69-74.
14. J. R. Jennings, A. Ghicov, L. M. Peter, P. Schmuki and A. B. Walker, *Journal of the American Chemical Society*, 2008, **130**, 13364-13372.
15. A. Y. Anderson, P. R. F. Barnes, J. R. Durrant and B. C. O'Regan, *The Journal of Physical Chemistry C*, 2011, **115**, 2439-2447.